3D Hierarchically Ordered Composite Block Copolymer Hollow Sphere Arrays by Solution Wetting

ARTICLE · DECEMBER 2010

Source: OAI

5 AUTHORS, INCLUDING:

Jun Fu
Ningbo Institute of Materials Technology an…
74 PUBLICATIONS **1,774** CITATIONS
SEE PROFILE

Dong Ha Kim
Ewha Womans University
136 PUBLICATIONS **3,158** CITATIONS
SEE PROFILE

Langmuir
Article
pubs.acs.org/Langmuir

3D Hierarchically Ordered Composite Block Copolymer Hollow Sphere Arrays by Solution Wetting

Jun Fu,*[,†,‡] Jianjun Wang,*[,†] Qin Li,[§] Dong Ha Kim,*[,∥] and Wolfgang Knoll[†,⊥]

[†]*Max Planck Institute for Polymer Research, Ackermannweg 10, Mainz 55128, Germany,* [‡]*Polymers and Composites Division, Ningbo Institute of Material Technology and Engineering, Chinese Academy of Sciences, 519 Zhuangshi Road, Zhenhai District, Ningbo, Zhejiang 315201, China,* [§]*Department of Chemical Engineering, Curtin University of Technology, Perth WA 6845, Australia,* [∥]*Department of Chemistry and Nano Science, Ewha Womans University, 11-1 Daehyun-dong, Seodaemun-gu, Seoul 120-750, Korea, and* [⊥]*Austrian Institute of Technology*

Received April 22, 2010. Revised Manuscript Received May 26, 2010

Hierarchically ordered 3D arrays of block copolymer hollow spheres have been fabricated by using solution wetting of silica inverse colloidal crystals. Subsequent drying and annealing in the molten state yield nanopatterned shells due to the microphase separation of the block copolymers. The shell thickness can be controlled by properly selecting the polymer solution concentration, and the nanostructures inside the shells can be manipulated by varying molecular weights and/or compositions of the block copolymers. This versatile strategy can be readily applied to fabricate patterned metal (gold and palladium) nanoparticles inside the shells of the highly ordered hollow spheres. Thus, the locally ordered nanostructures of block copolymers are integrated into long-range 3D order defined by the silica inverse colloidal crystal templates, promising convenient fabrication of highly integrated devices.

Introduction

Hollow spheres of silica,[1−4] oxides,[5,6] metals,[7,8] semiconductors,[9,10] carbon,[11,12] polymers,[12,13] and nanoparticle/polymer composites[14,15] with well-defined nanostructures have been attracting increasing research enthusiasm due to their potential applications for controlled release,[3] catalysis,[8,11] separation, photonic band gap,[16] mechanosensors,[17] biological devices, etc.[18] Numerous template-based approaches have been developed to fabricate such hollow spheres, including in situ synthesis,[17] surface polymerization,[19] and layer-by-layer assembly.[20] For example, hollow spherical silica materials with mesoporous walls have been successfully fabricated by the dual templating method where sacrificial spheres are used to template hollow spheres and a surfactant[4,21] or copolymer[3,12] is used to direct ordered mesoporous silica walls from precursor solutions. Monodisperse hollow spheres can further form three-dimensional (3D) ordered macroporous structures[13] with embedded mesoscale features on the cavity walls, yielding 3D arrays with hierarchical orders.[11,12] Colloidal templating has been an excellent platform for creating hierarchically ordered porous materials[22] and inverse colloidal crystals with mesoscale features in the walls afforded by copolymers or surfactants.[23] In this paper we report a versatile strategy of using silica inverse colloidal crystals (ICC) as a template for fabricating 3D hierarchically ordered block copolymer hollow sphere arrays which renders a great flexibility in mesoscale functionalization.

In contrast to the abundant studies on hollow spheres of silica and other inorganic materials with hierarchical orders, nanostructured hollow spheres of block copolymers (BCP) are rarely reported, and there are no reports on highly ordered 3D arrays of nanostructured hollow spheres of BCPs and composites. BCP-based 3D arrays of hollow spheres will allow for flexibility, versatility, and/or multifunctionality. In thin films, the microphase-separated (MPS) nanopatterns of BCPs[24] provide ideal

*Corresponding authors. E-mail: fujun@nimte.ac.cn (J.F.); wangj@mpip-mainz.mpg.de (J.W.), dhkim@ewha.ac.kr (D.H.K.).

(1) Sun, Q.; Kooyman, P. J.; Grossmann, J. G.; Bomans, P. H. H.; Frederik, P. M.; Magusin, P. C. M. M.; Beelen, T. P. M.; van Santen, R. A.; Sommerdijk, N. A. J. M. *Adv. Mater.* **2003**, *15*, 1097–1100.
(2) Sen, T.; Tiddy, G. J. T.; Casci, J. L.; Anderson, M. W. *Chem. Mater.* **2004**, *16*, 2044–2054.
(3) Botterhuis, N. E.; Sun, Q.; Magusin, P. C. M. M.; van Santen, R. A.; Sommerdijk, N. A. J. M. *Chem.—Eur. J.* **2006**, *12*, 1448–1456.
(4) Li, F.; Wang, Z.; Ergang, N. S.; Fyfe, C. A.; Stein, A. *Langmuir* **2007**, *23*, 3996–4004.
(5) Li, H.; Ha, C.-S.; Kim, I. *Langmuir* **2008**, *24*, 10552–10556.
(6) Zhong, Z.; Yin, Y.; Gates, B.; Xia, Y. *Adv. Mater.* **2000**, *12*, 206–209.
(7) Cong, H.; Cao, W. *J. Colloid Interface Sci.* **2004**, *278*, 423–427.
(8) Kim, S.-W.; Kim, M.; Lee, W. Y.; Hyeon, T. *J. Am. Chem. Soc.* **2002**, *124*, 7642–7643.
(9) Ma, Y.; Qi, L.; Ma, J.; Cheng, H.; Shen, W. *Langmuir* **2003**, *19*, 9079–9085.
(10) Son, D.; Wolosiuk, A.; Braun, P. V. *Chem. Mater.* **2009**, *21*, 628–634.
(11) Chai, G. S.; Shin, I. S.; Yu, J.-S. *Adv. Mater.* **2004**, *16*, 2057.
(12) Wang, Z.; Kiesel, E. R.; Stein, A. *J. Mater. Chem.* **2008**, *18*, 2194–2200.
(13) Xu, X.; Asher, S. A. *J. Am. Chem. Soc.* **2004**, *126*, 7940–7945.
(14) Qiao, R.; Zhang, X. L.; Qiu, R.; Kim, J. C.; Kang, Y. S. *Chem. Mater.* **2007**, *19*, 6485–6491.
(15) Wong, M. S.; Cha, J. N.; Choi, K.-S.; Deming, T. J.; Stucky, G. D. *Nano Lett.* **2002**, *2*, 583–587.
(16) Jiang, P.; Bertone, J. F.; Colvin, V. L. *Science* **2001**, *291*, 453–457.
(17) Arsenault, A. C.; Clark, T. J.; von Freymann, G.; Cademartiri, L.; Sapienza, R.; Bertolotti, J.; Vekris, E.; Wong, S.; Kitaev, V.; Manners, I.; Wang, R. Z.; John, S.; Wiersma, D.; Ozin, G. A. *Nature Mater.* **2006**, *5*, 179–184.
(18) Dersch, R.; Steinhart, M.; Boudriot, U.; Greiner, A.; Wendorff, J. H. *Polym. Adv. Technol.* **2005**, *16*, 276–282.
(19) Chen, Y. W.; Kang, E. T.; Neoh, K. G.; Greiner, A. *Adv. Funct. Mater.* **2005**, *15*, 113–117.
(20) Caruso, F. *Top. Curr. Chem.* **2003**, *227*, 145–168.
(21) Djojoputro, H.; Zhou, X. F.; Qiao, S. Z.; Wang, L. Z.; Yu, C. Z.; Lu, G. Q. *J. Am. Chem. Soc.* **2006**, *128*, 6320–6321.
(22) Li, Q.; Retsch, M.; Wang, J.; Knoll, W.; Jonas, U. *Top. Curr. Chem.* **2009**, *287*, 135–180.
(23) Yang, P.; Deng, T.; Zhao, D.; Feng, P.; Pine, D.; Chmelka, B. F.; Whitesides, G. M.; Stucky, G. D. *Science* **1998**, *282*, 2244–2246.
(24) Hamley, I. W. *The Physics of Block Copolymers*; Oxford University Press: Oxford, 1998; p 432.

Scheme 1. Schematic Representation of the Solution Wetting Method To Fabricate 3D Arrays of Hollow Spheres of Block Copolymers and Composites

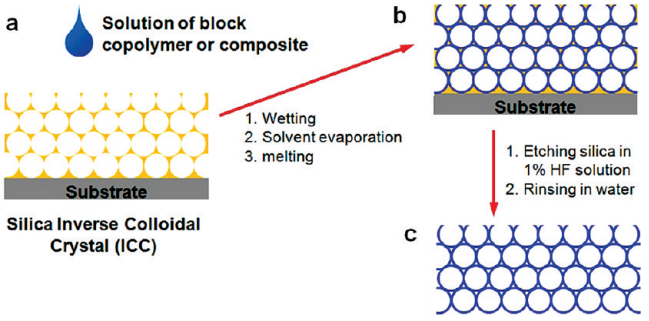

templates for the patterning of nanoparticles,[25,26] proteins,[27] or synthesis of nanofibrils.[28] When integrated into macroscale ordered structures (e.g., micropatterns[29−31] or nanopores[32,33]), BCPs gain both local order and large-scale order which is usually not available to BCPs alone. Hierarchical orders have been widely achieved in the arrays of nanofilaments,[32,33] patterned and confined thin films,[29−31] and solid spheres.[34−36] In those cases, the orientation of the MPS nanopatterns can be delicately controlled by deliberate alternation of the copolymer wetting nature with the surface-modified templates.[35] One exciting route to BCP-based devices is creating 3D arrays of BCP hollow spheres that contain large specific surface area and high density of reactive sites by integration of metal nanoparticles and/or functional groups. The orientation or ordering of the BCP nanostructures is also critical to the performances of devices based on such hierarchically ordered 3D arrays.

In this paper, we demonstrate a facile and versatile method to fabricate highly ordered 3D arrays of hollow spheres of BCPs and nanoparticle/BCP composites with nanostructured shells and nanopatterns at the inner surface. Silica inverse colloidal crystals (ICC) were used as templates that were wetted with solutions of BCPs and composites. After solvent evaporation, the wetting layers were annealed to form thermally equilibrated well-defined nanopatterns through MPS. After removing the silica ICC templates, free-standing 3D arrays of hollow BCP spheres with nanostructured shells were obtained. This procedure is depicted in Scheme 1 and was generalized to the fabrication of highly ordered 3D arrays of different BCPs and their composites with metal nanoparticles.

Table 1. Characteristics of Block Copolymers Used in This Work[a]

block copolymer	polymer code	M_n[b] (kg/mol)	W_{PS}[c]	M_w/M_n
PS-*b*-PMMA	S_{326}-MMA_{301}	64	0.53	1.09
	S_{450}-MMA_{182}	66	0.72	1.06
	S_{796}-MMA_{322}	115	0.72	1.04
	S_{1037}-MMA_{322}	140	0.77	1.07
PS-*b*-P2VP	S_{528}-$2VP_{177}$	73.5	0.75	1.06

[a] All data are provided by Polymer Source Inc., Canada. [b] Number-average molecular weight. [c] Weight fraction of polystyrene.

Experiments

Monodisperse PS microspheres with a diameter of 620 nm were prepared by emulsion polymerization[37,38] and purified by several cycles of centrifugation and redispersion in Milli-Q water (Millipore GmbH, Eschborn, Germany). The particle size was measured by dynamic light scattering with a Zeta Sizer 3000HS (Malvern Instrument Ltd.). Silica nanoparticles (diameter of 10 nm) were obtained from EKA Chemicals. Cotransfer of a mixture suspension with PS microspheres and silica nanoparticles led to multilayered binary colloid crystal films. The composite films were tempered at 450 °C in air to remove the PS and sinter the silica nanoparticle matrix, yielding silica inverse opals.[37,38]

Block copolymers (polystyrene-*block*-poly(methyl methacrylate), PS-*b*-PMMA, and PS-*b*-poly(2-vinylpyridine), PS-*b*-P2VP) used in this study (Table 1) were purchased from Polymer Source Inc., Canada, and used as received. The powders were dissolved in toluene or chloroform to make solutions with polymer concentrations from 0.25 to 2 wt %.

To make nanoparticle/block copolymer composite solutions, hydrogen tetrachloroaurate ($HAuCl_4$) and palladium hexafluoroacetylacetonate ($Pd(hfac)_2$) were mixed with PS-*b*-P2VP and PS-*b*-PMMA solutions under stirring, respectively. Both $Pd(hfac)_2$ and $HAuCl_4$ were purchased from Sigma-Aldrich and used as received.

Several drops of a solution were cast onto a silica ICC film to wet the silica walls. The solvent evaporated spontaneously, leaving block copolymer thin films on the silica wall. Subsequently, the BCP-loaded template was annealed in vacuum at 200 °C for 24 h in order to approach equilibrium MPS or nanoparticle reduction and assembling. Finally, the sample was cooled to room temperature in vacuum before they were taken out of the oven.

In order to remove the silica templates, the BCP/silica composites were immersed in 1% HF/water solution overnight. (*Caution*: HF is harmful and should be handled under proper protection and in a fume hood!) Block copolymer films were floated on water surface and picked up with clean glass slides or silicon wafers. The films were completely rinsed with deionized water for several times and then dried in vacuum at 60 °C overnight.

The morphologies and structures of the templates and the resulting block copolymer hollow sphere arrays were investigated with a LEO Gemini 1530 field emission scanning electron microscope at acceleration voltage of 1 kV on native samples. No sputtering was necessary to make the samples conductive.

Results and Discussion

Silica inverse colloidal crystals (ICC) with pore diameter of 620 nm and interconnecting voids (Figure 1a)[37,38] were employed as templates for the fabrication of 3D arrays of BCP and composite hollow spheres. Under appropriately controlled experimental conditions, the number of layers in the colloidal crystals and the ICCs varied from one up to tens of layers.[39,40]

(25) Horiuchi, S.; Sarwar, M. I.; Nakao, Y. *Adv. Mater.* **2000**, *12*, 1507–1511.
(26) Kim, D. H.; Jia, X. Q.; Lin, Z. Q.; Guarini, K. W.; Russell, T. P. *Adv. Mater.* **2004**, *16*, 702–+.
(27) Lau, K. H. A.; Bang, J.; Kim, D. H.; Knoll, W. *Adv. Funct. Mater.* **2008**, *18*, 3148–3157.
(28) Li, X.; Tian, S.; Ping, Y.; Kim, D. H.; Knoll, W. *Langmuir* **2005**, *21*(21), 9393–9397.
(29) Stoykovich, M. P.; Muller, M.; Kim, S. O.; Solak, H. H.; Edwards, E. W.; de Pablo, J. J.; Nealey, P. F. *Science* **2005**, *308*, 1442–1446.
(30) Cheng, J. Y.; Ross, C. A.; Smith, H. I.; Thomas, E. L. *Adv. Mater.* **2006**, *18*, 2505–2521.
(31) Pai, R. A.; Humayun, R.; Schulberg, M. T.; Sengupta, A.; Sun, J.-N.; Watkins, J. J. *Science* **2004**, *303*, 507–510.
(32) Wu, Y.; Cheng, G.; Katsov, K.; Sides, S. W.; Wang, J.; Tang, J.; Fredrickson, G. H.; Moskovits, M.; Stucky, G. D. *Nature Mater.* **2004**, *3*, 816–822.
(33) Shin, K.; Xiang, H.; Moon, S. I.; Kim, T.; McCarthy, T. J.; Russell, T. P. *Science* **2004**, *306*, 76.
(34) Arsenault, A. C.; Rider, D. A.; Ttreault, N.; Chen, J. I. L.; Coombs, N.; Ozin, G. A.; Manners, I. *J. Am. Chem. Soc.* **2005**, *127*, 9954–9955.
(35) Rider, D. A.; Chen, J. I. L.; Eloi, J.-C.; Arsenault, A. C.; Russell, T. P.; Ozin, G. A.; Manners, I. *Macromolecules* **2008**, *41*, 2250–2259.
(36) Higuchi, T.; Tajima, A.; Motoyoshi, K.; Yabu, H.; Shimomura, M. *Angew. Chem., Int. Ed.* **2009**, *48*, 5125–5128.
(37) Wang, J.; Li, Q.; Knoll, W.; Jonas, U. *J. Am. Chem. Soc.* **2006**, *128*, 15606–15607.
(38) Wang, J.; Ahl, S.; Li, Q.; Kreiter, M.; Neumann, T.; Bukert, K.; Knoll, W.; Jonas, U. *J. Mater. Chem.* **2008**, *18*, 981–988.
(39) Jiang, P.; Bertone, J. F.; Hwang, K. S.; Colvin, V. L. *Chem. Mater.* **1999**, *11*, 2132–2140.
(40) Li, J.; Han, Y. *Langmuir* **2006**, *22*, 1885–1890.

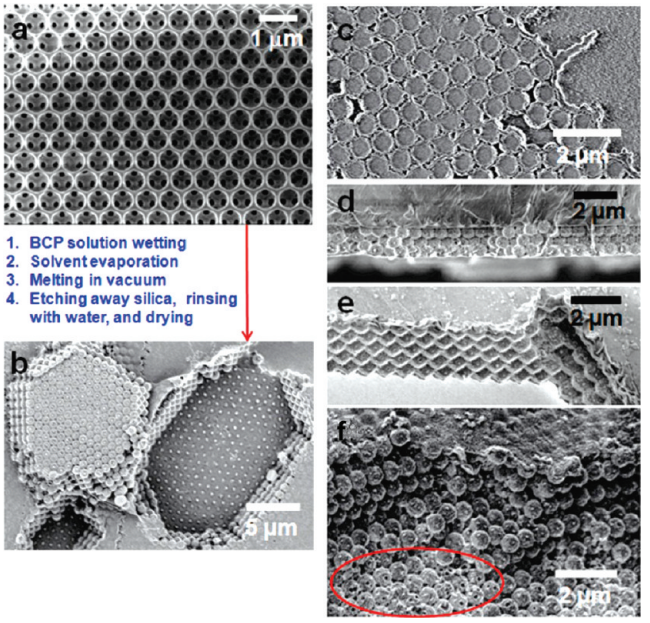

Figure 1. SEM images of (a) the silica inverse colloidal crystal fabricated by cotransfer of 620 nm PS spheres and silica nanoparticles and subsequent sintering at 450 °C. After solution wetting, solvent evaporation, melting in vacuum, and removal of silica templates, free-standing films with (b) 4, (c) 1, (d) 3 (e) 5, and (f) over 10 layers of PS-*b*-PMMA hollow sphere arrays were obtained.

In a representative experiment, a symmetric polystyrene-*block*-poly(methyl methacrylate) (S_{326}-MMA_{301}, Polymer Source, Inc., Canada, Table 1) copolymer was dissolved in toluene with polymer concentration of 1.0 wt %. Several drops of solutions were cast onto silica ICC, and then the solvent evaporated spontaneously. Subsequently, the sample was annealed at 200 °C for 24 h in vacuum to approach equilibrium microphase separation. Finally, the samples were immersed in 1% hydrofluoric (HF) acid solution overnight to remove silica. (*Caution*: HF is harmful and should be handled under proper protection and in a fume hood!) After complete rinsing with deionized water for several times, the silica template was removed and free-standing BCP film was floated in water (Figure 1). The film was picked up with a clean glass slide.

The BCP films without metal sputtering were imaged by using a field emission scanning electron microscope (SEM, FEI/Philips) at 1 kV. Representative SEM images of the resulted arrays of PS-*b*-PMMA spheres are presented in Figure 1b−f. These spheres appeared as perfect negative replicates of the silica ICC templates. Mass transport through the cavities between the air voids in the silica ICC enables a complete wetting of the silica walls by the solutions. These copolymer spheres formed shared necks with each other (Figure S1), and as represented below, these spheres are hollow with nanostructured shells after melted within the templates at high temperatures. The packing geometry and the number of layers are identical to those of the original PS colloidal crystals. By using PS colloidal crystals with different thicknesses, we have successfully fabricated S_{326}-MMA_{301} hollow sphere arrays with 1, 3, 4, 5, and tens of layers (Figure 1b−f). The average sphere diameters and center-to-center distances were 620 nm, identical to the average diameter of the initial PS spheres. This solution wetting method allows for the fabrication of 3D sphere arrays with any packing geometries defined by the templates. In the area highlighted by the red oval in Figure 1f, one can observe 3-fold pores on the replica spheres, which shows that the spheres are hollow and interconnected. More evidence of the hollow sphere morphology is shown in Figure S2.

Different from the solid block copolymer spheres fabricated from very concentrated block copolymer solutions after slow solvent evaporation by Manners and co-workers,[35] these hollow spheres are unique since our solution wetting method generates thin layers of block copolymer solutions on the silica walls of ICC templates and thus creates thin block copolymer films on the internal surface of templates after solvent evaporation, leading to the formation of hollow block copolymer spheres. Thus, the well-known microphase-separated nanostructures of block copolymers in thin films and/or bulk are integrated into curved surface with curvatures tunable by changing the pore size of template particles. Also different from the solid spheres is that the additional inner surface of the hollow spheres may provide functional sites with high integration, which is crucial for sensors or devices.

The shell thickness of these hollow spheres depended on the solution concentration (Figure 2a). From 0.25 wt % PS-*b*-PMMA/toluene solution, the wall thickness was ~33 nm. As the concentration was increased to 0.5, 1.0, and 2.0 wt %, the shell thickness increased to ~50, 73, and 100 nm.

Figure 2b shows a representative 3D array of hollow PS-*b*-PMMA spheres after removal of silica templates. The internal surface structures were observed by SEM of the hemispheres formed in the opening of the silica ICC templates (schemes of the openings are inserted to Figure 2c,g). Since the PMMA chains are prone to degradation upon exposure to electron beam, the PS-rich domains appear bright and the PMMA-rich domains appear dark. Before annealing, no MPS structures were formed (Figure S3). MPS took place during melting the hollow spheres in silica ICC templates at 200 °C for 24 h in a vacuum. In melt, the preferential affinity of PMMA to the silica walls[41] drives the formation of a single PS-*b*-PMMA layer at the polymer/silica interface (which became the outer surface of the hollow spheres after silica removal, as schemed in Figure 2d,f,g). At 200 °C, the surface tension difference between PS and PMMA vanishes so as to allow for perpendicular orientation[42,43] of the PS-*b*-PMMA nanopatterns on this single layer in the PS-*b*-PMMA shells.

Figure 2c shows the perpendicular S_{326}-MMA_{301} lamellae with respect to the shell surface, and this morphology is schematically illustrated in Figure 2d. The apparent lamella period is ~32 nm, smaller than the bulk value (38.5 nm). Besides, the apparent PS fraction appeared larger than the PMMA fraction at surface, deviating from the expected symmetric lamellae. The curvature of the spheres and the attraction from the silica surface to PMMA may account for this deviation. Such deviation is more profound for the asymmetric PS-*b*-PMMA in the shells. Figure 2e shows representative patterns in a hollow sphere of S_{450}-MMA_{182}, which in bulk normally forms PMMA cylinders in the PS matrix. In the shell, short PS rods were found instead of PMMA cylinders, presumably due to the migration of PMMA to the silica wall. Besides, the majority of the internal surface was covered with PS (Figure 2f). The PS migration to the surface became more profound as the M_n was increased to 115 kg/mol (S_{796}-MMA_{322}, $W_{PS} \approx 0.72$) and 140 kg/mol (S_{1037}-MMA_{322}, $W_{PS} \approx 0.77$). An example of a S_{1037}-MMA_{322} pore is shown in Figure 2g, where the majority of the internal surface is occupied by PS while highly ordered PMMA spheres instead of cylinders were visible at the surface (Figure 2h). Note that the apparent period of these spheres (~33 nm) is smaller than that of bulk S_{1037}-MMA_{322}.

(41) Fasolka, M. J.; Mayes, A. M. *Annu. Rev. Mater. Res.* **2001**, *31*, 323.
(42) Wu, S. In *Polymer Handbook*, 4th ed.; Brandrup, J., Immergut, E. H., Grulke, E. A., Eds.; Wiley-Interscience: New York, 1999; Vol. *2*.
(43) Sivaniah, E.; Hayashi, Y.; Matsubara, S.; Kiyono, S.; Hashimoto, T.; Fukunaga, K.; Kramer, E. J.; Mates, T. *Macromolecules* **2005**, *38*, 1837–1849.

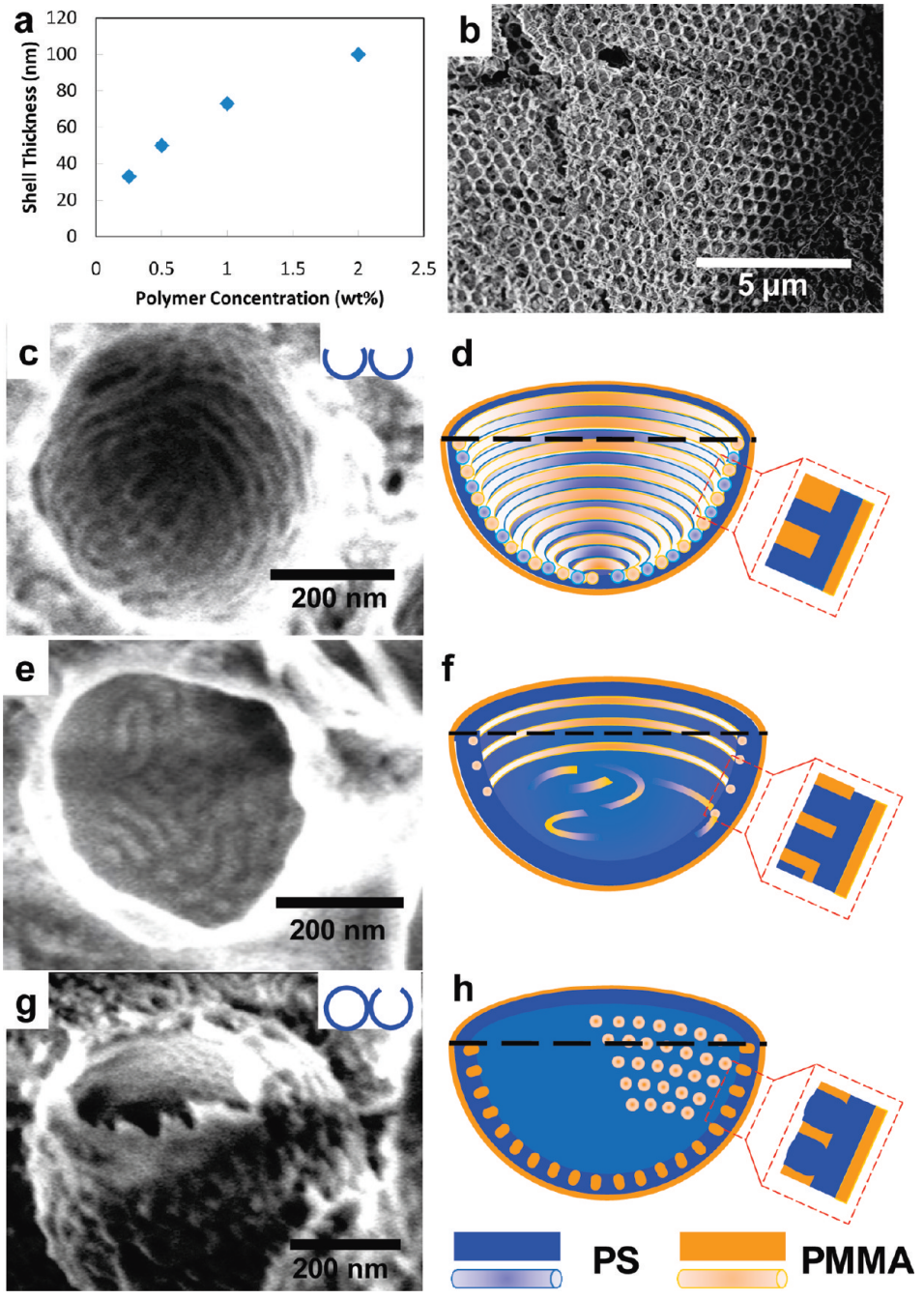

Figure 2. (a) Concentration dependence of shell thickness and the SEM images of, after removal of silica templates, (b) the 3D arrays of hollow PS-*b*-PMMA spheres and the annealed hollow spheres of (c) S_{326}-$PMMA_{301}$, (e) S_{450}-MMA_{182}, and (g) S_{1037}-MMA_{322}. The PS-rich domains appear bright and the PMMA-rich domains appear dark in the SEM images. The schemes in (d), (f), and (h) represent the schematic cross-section view of the nanostructured shells observed in (c), (e), and (g).

Herein, the coexistence of polymer/silica and polymer/vacuum interfaces in the shells of the hollow spheres differs from our results from the solid structures of BCPs under confinements in nanotubes,[32,33] particles,[36,44] or colloidal crystals.[34] The shell structures in this work defined by these interfacial interactions are schematically illustrated in Figure 2d,g,h. The BCP nanopatterns at the inner surface of shells are unique and can be adjusted by changing the commensurability between the BCP period and the shell geometry.

To examine the confinement effect on the self-assembly of symmetric diblock copolymers, we systematically varied the silica ICC pore diameters from 300, 270, to 235 nm. These pores possess a small fraction of the shells (Figure 3, bottom) so that the boundary effect dominates the lamella orientation. According to the perpendicular lamellae of the symmetric S_{326}-MMA_{301} film at a glass slide surface, its average period (L_0) is about 38.5 nm (Figure 3a). As this symmetric PS-*b*-PMMA was confined in silica pores, the preferential affinity of the PMMA blocks to the silica walls induced an orientation of lamellae along the contour of the pores. Inside these pores, the copolymer chains adjust their conformation and period in order to be commensurate with the pore size. As a result, the pore diameters (D_p) are scaled by the adjusted lamellar period (L): As D_p was 300 nm (Figure 3b) or $7.8L_0$, the PS-*b*-PMMA lamellae expanded to a period (L) of

(44) Lu, Y.; Fan, H.; Stump, A.; Ward, T. L.; Rieker, T.; Brinker, C. J. *Nature* **1999**, *398*, 223–226.

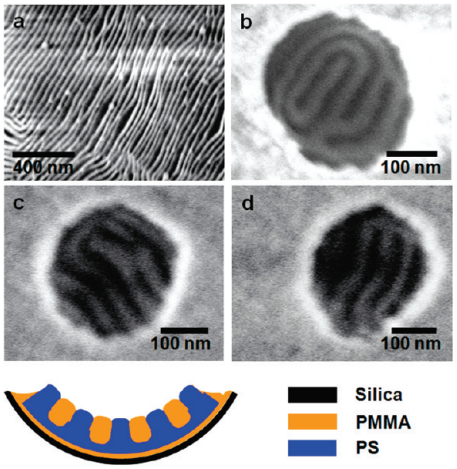

Figure 3. SEM images of (a) perpendicular lamellae of a symmetric S_{326}-MMA_{301} and the lamellae confined in silica pores with diameters of (b) 300, (c) 270, and (d) 235 nm. The scheme at the bottom presents a schematic illustration of a cross-section view of the block copolymer shell.

46 nm so that $D_p = 6.5L$. Similarly, as D_p was 270 nm ($7.0L_0$, Figure 3c) and 235 nm ($6.1L_0$, Figure 3d), L became 48.9 nm ($D_p = 5.5\,L$) and 52 nm ($D_p = 4.5\,L$), respectively. Thus, the pore diameters were scaled as $(n + 1/2)L$ so as to fulfill the boundary condition. Similar readjustment of copolymer period for quantization of confinement geometry has been reported for BCP confined in nanopores[32,33] and solid copolymer particles.[34] In hollow spheres, the presence of an additional free surface (polymer/vacuum interface) can make the confinement more complicated: the shell thickness and the curvature, in addition to the polymer/silica interfacial interactions, will contribute to the formation and orientation of the MPS nanopatterns.

Different from homopolymer or elastomer hollow spheres[17] inverse colloidal crystals, integration of MPS nanostructures into 3D ordered macroporous by using BCPs is advantageous for the nanoscale selectivity when functionalized with specific species such as nanoparticles, proteins,[27] or small molecules. Further, the fabrication of the arrays of hollow block copolymer structures[35] in inverse colloidal crystals allows for mass transport through the submicromter pores and thus is promising for fabrication of devices or sensors with high sensitivity, which is usually not available for the solid block copolymer structures templated in inverse colloidal crystals.[35]

We demonstrated the fabrication of hollow spheres of gold nanoparticle/BCP composites. $HAuCl_4$ was mixed with PS_{528}–$P2VP_{177}$ ($W_{PS} = 0.75$, the molar ratio of $HAuCl_4$ and pyridine moieties was 1:5) in 1.0 wt % chloroform solution. In solution, the pyridine moieties complexed with $HAuCl_4$ and the latter was gradually reduced into gold nanoparticles (Au-NP). This composite solution was cast on silica ICCs to wet the template walls, forming a thin layer of Au-NP/PS-*b*-P2VP composite (Figure 4a). The Au-NPs were embedded in the polymer matrix and did not show any order (Figure 4b). After annealing within the silica template at 200 °C for 24 h in vacuum, the number density of Au-NPs was substantially increased and the Au-NPs exhibited ordered arrangement (Figure 4c). The gold nanoparticles prefer to segregate to the free surface at 200 °C (Figure 4c). These locally ordered Au NPs were also arranged into long-range order defined by the silica ICC templates. Thus, the nanopatterned Au NPs are integrated into long-range orders that are not available for nanoparticles or block copolymers alone. Such hierarchically ordered spatial distribution may produce localized surface plasmonic effect.[38]

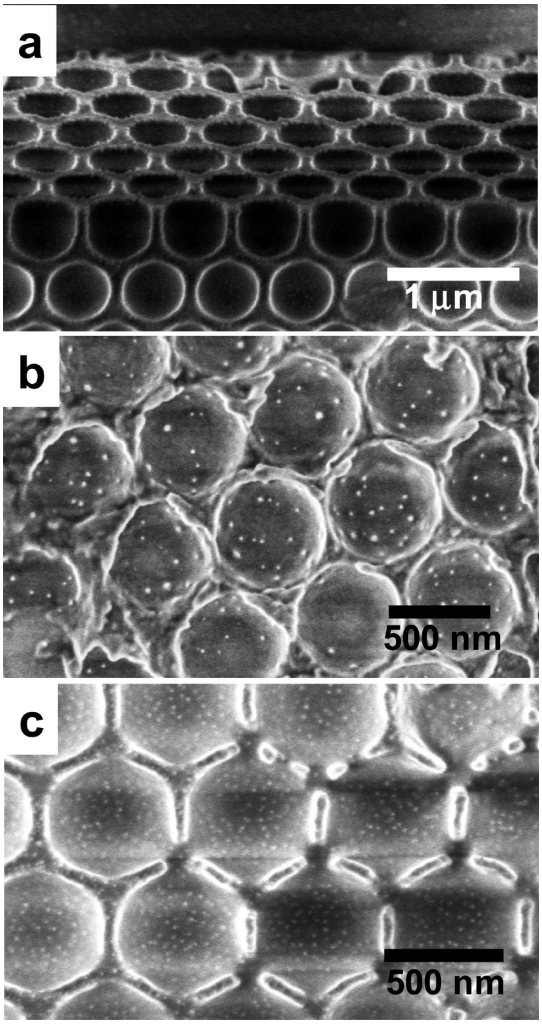

Figure 4. SEM images of Au/PS-P2VP hemisphere array (a) with silica templates (side view); (b) before and (c) after annealing at 200 °C for 24 h and with subsequent removal of silica templates.

This strategy was also applied to fabricate composite hollow spheres with patterned palladium (Pd) nanoparticles. By using palladium hexafluoroacetylacetonate/S_{326}-MMA_{301} solution in toluene with a Pd:styrene molar ratio of 1:10 to wet the silica ICC template, we obtained hollow spheres of Pd/PS-*b*-PMMA composite after drying and annealing at 200 °C for 24 h in vacuum. During annealing, Pd(II) ions migrated to and were preferentially reduced into Pd nanoparticles in PS domains.[25,45] This reduction and growth process led to ripening of Pd nanoparticles that were arranged along the PS nanodomains (Figure S4).

Conclusions

We have demonstrated a general template-based fabrication of 3D arrays of hollow spheres of block copolymers and composites. By wetting silica inverse colloidal crystals with block copolymer solutions, hollow spheres of block copolymers were obtained after solvent evaporation. The shells of such hollow spheres contained microphase-separated nanostructures after annealing at elevated temperatures. This method can be utilized to fabricate 3D arrays of nanoparticle/copolymer composites with hierarchical orders. The combination of ordered macro- and mesostructures is

(45) Horiuchi, S.; Fujita, T.; Hayakawa, T.; Nakao, Y. *Langmuir* **2003**, *19*, 2963–2973.

promising for the creation of novel functional materials and/or highly integrated devices, of which both the structures and functionality can be controlled.

Acknowledgment. J.F. thanks the Max Planck Society fellowship. Q.L. is grateful to the financial support from the Australian Research Council (ARC DP0558727). D.H.K. was supported by National Research Foundation of Korea Grant funded by the Korean Government (Nos. 20090063000 and R01-2008-000-11712-0).

Supporting Information Available: More SEM images (Figures S1−S4). This material is available free of charge via the Internet at http://pubs.acs.org.